Design of Ultra-Thin InP Solar Cell Using Carrier Selective Contacts

Vidur Raj, *Member*, IEEE, Fiacre Rougieux, *Member, IEEE*, Lan Fu, *Senior Member*, IEEE, Hark Hoe Tan, *Fellow*, IEEE, Chennupati Jagadish, *Fellow*, IEEE

***Abstract*— Most recently, III-V based ultra-thin solar cells have attracted much attention for their inherent advantages such as increased tolerance to defect recombination, efficient charge carrier separation, photon recycling, flexibility, and reduced material consumption. However, so far, almost all reported devices make use of conventional doped p-i-n kind of structures with a wide bandgap III-V lattice-matched epitaxial window layer, for passivation and reduced contact recombination. Here, we show that a high-efficiency device can be obtained utilizing an InP thin film of thickness as low as 280 nm, without the requirement of a conventional p-n homojunction or epitaxial window layer. This is achieved by utilizing a wide bandgap electron and hole selective contacts for electrons and holes transport, respectively. Under ideal conditions (assuming Interface Recombination Velocity (IRV) = 10^3 cm/s and bulk lifetime =1 us), the proposed solar cell structure can achieve efficiency as high as 28%. Although, in the presence of bulk and interface SRH recombination, the efficiency reduces, still for bulk minority carrier lifetime as low as 2ns and an IRV as high as 10^5 cm/s, an efficiency of ~22% can be achieved with InP thickness as low as 280 nm. The proposed device structure will be beneficial in cases where the growth of controlled p-n homojunction and window layer can be tedious as in case of low-cost deposition techniques, such as thin-film vapour-liquid-solid (TF-VLS) and close-spaced vapour transport (CSVT).**

***Index Terms*— Carrier selective contacts, Heterocontacts, Optoelectronic Simulation, III-V Photovoltaics, FDTD, TCAD**

I. Introduction

EVEN though III-V semiconductors such as InP and GaAs have near optimum bandgap for high-efficiency solar cells, they are not widely used as a solar cell material for commercial applications [1-3]. This is mainly due to the high cost of III-V solar cells. The high cost of III-V solar cells is a result of costly substrate requirement for epitaxial growth as well as the high processing cost involved in the fabrication of these cells [3-5]. Nonetheless, III-V semiconductors have great potential to achieve low cost, if the problem of the high cost of the substrate and absorber layer can be addressed without compromising its high efficiency [3, 5]. One of the best examples of such affordable and efficient devices is the flexible solar cells commercially available from “Alta Devices” [6]. III-V solar cells from Alta Devices incorporate epitaxial lift-off technology to reduce the substrate cost [7, 8]. Though epitaxial lift-off has been able to reduce the overall cost of III-V solar cells, it is still significantly more expensive than commercial silicon solar cells [9].

Most recently, researchers have started looking into the development of ultra-thin solar cells based on III-V semiconductors [10-14]. For example, in a very recent report, Ling et al. reported an untra-thin GaAs solar cell with 19.9% efficiency [14]. Ultra-thin solar cells are usually only few hundred nanometers thick and have several advantages such as reduced material consumption, increased fabrication throughput, lower radiation damage, high defect tolerance, reduced bulk recombination, and photon recycling [10-13, 15-18]. So far, researchers have only used conventional solar cell structures for fabrication of these ultra-thin III-V solar cells. In a conventional solar cell structure, a base (intrinsic) layer is sandwiched between heavily doped n^+ and p^+ layers to achieve charge carrier separation, along with a heavily doped wide bandgap window layer for surface passivation and carrier selectivity [10-13, 15-18]. These doped layers, along with the window layer, add to the complexity as well as the final cost of the III-V solar cell. Furthermore, despite being mainstream, these doped devices are not optimal and are hindered by several optoelectronic losses along with technological limitations specific to doped structures [1, 2, 19].

Furthermore, recent cost analysis of III-V solar cells shows that the high cost of III-V solar cell is mainly due to relatively costly epitaxial growth and processing of III-V solar cells along with maintenance of MOCVD (Metal-Organic Chemical Vapour Deposition) equipment [9, 20]. To overcome the cost limitations imposed by MOCVD based epitaxial growth, researchers have started looking into alternative growth techniques such as thin-film vapor-liquid-solid (TF-VLS) [21-23] and close-spaced vapor transport (CSVT) [24, 25]. These

This research is supported by the Australian Research Council.

(Corresponding Author: Vidur Raj and Hark Hoe Tan)

VR, LF, HT and CJ are with the Department of Electronic Materials Engineering, Research School of Physics and Engineering, The Australian National University, Canberra, ACT 2601, Australia (e-mail: vidur.raj@anu.edu.au; lan.fu@anu.edu.au; hoe.tan@anu.edu.au; chennupati.jagadish@anu.edu.au.)

FR is with School of Photovoltaic and Renewable Energy Engineering, University of New South Wales, Kensington, NSW 2052, Australia. (email: fiacre.rougieux@unsw.edu.au)

An electronic copy of the supporting information is available online or from the author.

Color versions of one or more of the figures in this paper are available online at http://ieeexplore.ieee.org

growth techniques are expected to lower the overall cost of III-V solar cell significantly. However, at present, these relatively nascent growth techniques face severe optimization challenges in achieving controlled p-n junction, doping, and growth of the window layer. These optimization problems can largely be solved by eliminating the requirement of a doped p-n junction.

In recent times, carrier selective contacts have emerged as an efficient alternative to doped junctions. For example, most recently, researchers have been able to fabricate silicon solar cells with efficiency exceeding 20% by replacing the p^+ and n^+ layers with hole and electron selective contacts, respectively [19, 26]. Though very well studied for silicon, reports on electron and hole selective contacts for III-V solar cells is somewhat limited, with only separate studies of electron or hole selective contacts for InP [1, 2, 27-29]. So far there are no reports on thin film InP solar cells where both electron and hole selective contact have been studied simultaneously.

In this work, we have performed a detailed optoelectronic simulation of an ultra-thin InP solar cell, where the p^+ and n^+ regions of the solar cell are replaced by the corresponding hole and electron selective contacts, respectively. Here, we utilize ZnO as an electron selective contact and copper iodide (CuI) as hole selective contact for InP, because they very well studied carrier selective contacts [1, 2, 30-35]. Our simulation results show that in the presence of a metal back reflector and an optimized front anti-reflection coating (MgF_2/ ITO/ZnO), a high short-circuit current (J_{sc}) of more than 28 mA/cm^2 can be achieved, for InP thickness as low as 280 nm. Note that in the absence of a metal back reflector and a front anti-reflection coating, the J_{sc} reduces to less than 19 mA/cm^2, for the 280 nm thick InP substrate. Furthermore, a 1-D device simulation performed on InP heterojunction solar cell (metal/ITO/ZnO/InP/CuI/metal) shows that under ideal conditions, efficiency of 26.1% and 27.6% can respectively be achieved, with and without photon recycling. Even for a bulk lifetime as low as 2 ns and a surface recombination velocity of less than 10^5 cm/s, an efficiency exceeding 22% can be achieved. Finally, we discuss the importance of the current work toward reducing the cost of III-V solar cells, while minimizing growth related complexities.

II. MODELING METHODS

A. FDTD Simulation

Optical simulation of the proposed solar cell was performed using a commercial FDTD package from Lumerical Inc.[36] FDTD (Finite-difference time-domain) is a numerical technique for solving Maxwell's equation in complex geometries for calculation of $E(\vec{r},\omega)$ (electric field) and $H(\vec{r},\omega)$ (magnetic field) at all points within the computational domain [1, 37]. The spatial $E(\vec{r},\omega)$ (electric field) and $H(\vec{r},\omega)$ (magnetic field) calculated using FDTD simulation can then be used to calculate the absorbed power as a function of space and angular momentum using the following equation:

$$P_{abs}(\vec{r},\omega) = \frac{1}{2}\,\omega\,|E(\vec{r},\omega)|^2 Im\{\epsilon(\vec{r},\omega)\} \qquad (1)$$

where P_{abs} is the power absorbed, ω is the angular frequency, $|E|^2$ is the electric field intensity, and $Im(\epsilon)$ is the imaginary part of the permittivity. In the ideal case, it can be assumed that for each absorbed photon, one electron-hole-pair is generated, and the generation rate in such cases is equivalent to the power absorbed (P_{abs}). Then, the generation rate, $G(\vec{r})$ for solar spectrum can be calculated by normalizing the absorbed power to the solar spectrum as

$$G(\vec{r}) \approx \int \frac{P_{abs}(\vec{r},\omega)\,.\,I_{solar}(\omega)}{I_{source}(\omega)}\,d\omega \qquad (2)$$

where $I_{solar}(\omega)$ and $I_{source}(\omega)$ are the solar (AM1.5) and source spectral irradiance, respectively. The ideal short circuit current, which is defined as the maximum achievable short-circuit current from a solar cell can be written in terms of $G(\vec{r})$ as:

$$J_{sc\,(ideal)} = \frac{e\int G(\vec{r}).\,dr}{A} \qquad (3)$$

Where, e is the electronic charge and A is the area of the solar cell. In this paper, $J_{sc\,(ideal)}$ is used as a performance parameter for optical optimization of the solar cells.

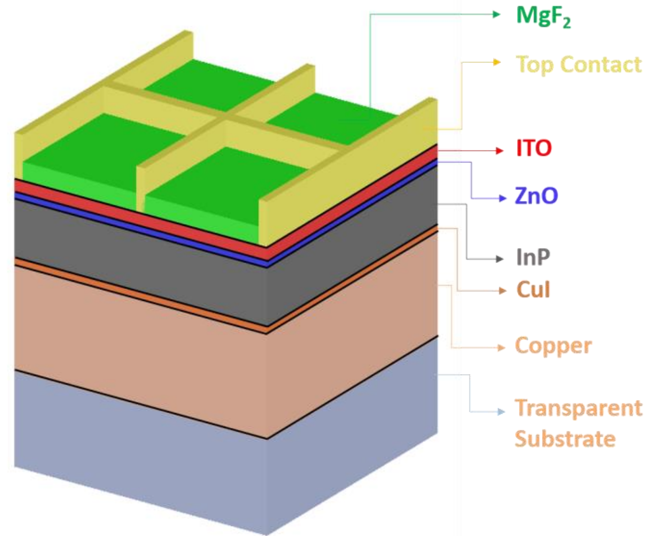

Fig. 1. 3-D schematic (not to scale) of proposed heterojunction solar cell. Interfaces between two materials are shown using a black line.

Figure 1 shows a 3-D schematic of the proposed solar cell. The proposed solar cell consists of an undoped InP absorber layer sandwiched between the electron (ZnO) and hole (CuI) selective contacts. Here, ITO functions as a transparent conductor, and the front metal contact is directly made on the ITO. For optical confinement in current solar cell, we use an optimum thickness of MgF_2/ITO/ZnO to reduce the reflection from the top surface along with a one μm-thick copper thin film at the bottom of the cell which acts as a back contact as well as a "metal back reflector". For FDTD simulations, the refractive index (n) and the extinction coefficient (k) of InP and copper were obtained from the software (Lumerical FDTD); however,

the n, k values for ZnO, CuI, MgF_2, and ITO were measured using an ellipsometer. The experimental values were then fitted using Lumerical's in-built analytical model and the best fit n, k values were used for performing the simulation. Figure S1 of the supplementary section shows experimental n, k values of different materials fitted using Lumerical's in-built fitting model. For simplicity, we fix the thickness of ZnO and CuI at 10 nm, while varying the thickness of ITO and MgF_2 to achieve minimum reflection from the top surface.

In general, SCAPS-1D has an in-built generation calculator; however, for solar cell structure, which involves complex optical behaviour, SCAPS-1D generation profile is not accurate. Therefore, we import the generation profile calculated using Lumerical FDTD to SCAPS-1D, to perform the device simulation. It is essential to mention that the mesh size of FDTD simulation and SCAPS-1D simulation were quite different, and therefore, the generation rate calculated using FDTD was interpolated at mesh points generated using SCAPS-1D.

TABLE I
MATERIAL PARAMETERS USED FOR DEVICE SIMULATIONS

	i-InP [34]	ZnO [2]	ITO [2]	γ-CuI [33, 35]
Thickness (nm)	280	10	60	10
Bandgap (eV)	1.344	3.4	3.65	3.1
Electron affinity (eV)	4.380	4.05	4.6	2.8
Dielectric permittivity (relative)	12.500	10	8.900	6.5
CB effective density of states ($1/cm^3$)	5.7×10^{17}	2.2×10^{18}	2×10^{18}	2.8×10^{19}
VB effective density of states ($1/cm^3$)	1.1×10^{19}	1.8×10^{19}	1.8×10^{19}	3.8×10^{20}
Electron thermal velocity (cm/s)	1×10^7	1.0×10^7	1.0×10^7	1×10^7
Hole thermal velocity (cm/s)	1×10^7	1.0×10^7	1.0×10^7	1×10^7
Electron mobility (cm^2/Vs)	1000	50	10	1
Hole mobility (cm^2/Vs)	400	1	1	5
Shallow uniform donor density (N_D) ($1/cm^3$)	1.0×10^{17}	1.0×10^{19}	1.0×10^{20}	1.0×10^7
Shallow uniform acceptor density (N_A) ($1/cm^3$)	1.0×10^7	1×10^7	1×10^7	1.0×10^{19}
RECOMBINATION PARAMETERS [34]				
Radiative recombination coefficient for InP			1.2×10^{10} cm^6/s	
Auger electron capture coefficient for InP			9×10^{-31} cm^6/s	
Auger hole capture coefficient for InP			9×10^{-31} cm^6/s	

B. Device Simulation

We used SCAPS-1D to perform 1-D device simulation of the solar cell structure shown in Figure 1. SCAPS-1D solves the drift-diffusion, continuity and Poisson's equations in 1-D to calculate the energy bands, carrier concentrations, J-V curve, and quantum efficiency at a given working point [38, 39]. The working point condition specifies the parameters, such as temperature, voltage, frequency, and the illumination, which cannot be varied during simulation but are relevant to create the output. Detailed mathematical and physics formalism of SCAPS-1D can be found in the supplementary section. The semiconductor input parameters and recombination parameters used during simulation are given in Table I. During device simulations we only simulate three fundamental recombination mechanisms including, radiative recombination, Auger recombination, and surface and bulk SRH recombination.

During all device simulation, we account for photon recycling effects. In general, the radiative recombination coefficient (B) is a material property and can be defined by Roosbroeck-Shockley relation as follows:

$$B = \frac{8\pi n^2}{n_i^2 c^2} \int_0^\infty \frac{\lambda^2 \alpha(\lambda)}{e^{\frac{hc}{\lambda kT}} - 1} d\lambda \quad (4)$$

where n is the refractive index of the absorber, n_i is the intrinsic carrier concentration of the absorber, c is the speed of light, $\alpha(\lambda)$ is the absorption coefficient as a function of wavelength (λ), k is the Boltzmann constant and T denotes the device temperature. In radiative recombination, an electron-hole-pair (e-h-p) recombines to emit a photon, and the photon escapes the cell through an escape cone. However, in the presence of photon recycling, the emitted photon is reabsorbed and remitted several times before it is lost through an escape

cone or non-radiative recombination. In the end, fractions of photons emitted during radiative recombination are reabsorbed to create more electron-hole-pairs [15, 42-44]. In other words, the net effect of photon recycling is a reduction in the rate of radiative recombination [42, 45]. Unlike radiative recombination, photon recycling is not only dependent on absorber material but is also dependent on solar cell structure, front and back reflectance, absorber layer thickness, doping, etc. [46, 47] Because of this complexity, the self-consistent solution to this process is very complicated. However, a straightforward way to incorporate photon recycling is to scale the radiative recombination coefficient by the recycling coefficient (Asbeck coefficient [48]) using the following relation [45]:

$$R_{recycle} \equiv \frac{R_{rad}}{\phi} \approx \frac{B}{\phi}\,(n.p - n_i^2) \qquad (5)$$

where $R_{recycle}$ is the effective radiative recombination rate after photon recycling, R_{rad} is the radiative recombination rate without photon recycling, ϕ is the recycling factor (Asbeck coefficient), n and p are the electrons and holes concentrations, respectively, and n_i is the intrinsic charge carrier concentration. The use of a recycling factor to account for photon recycling is a valid way to get the upper bound of the working of a given solar cell in presence of photon recycling and has readily been used by several of the authors.[46, 47, 49, 50] In the current scenario, we assume the radiative recombination coefficient of InP is 1.2×10^{-10} $cm^{-3}s^{-1}$, and we use the recycling factor values for n-type InP reported in ref [51]. We use a recycling factor corresponding to n-type InP because undoped InP grown using different techniques tends to have n-type background doping of the order of 1×10^{15}-1×10^{16} cm^{-3} due to silicon impurity.[22, 52, 53]

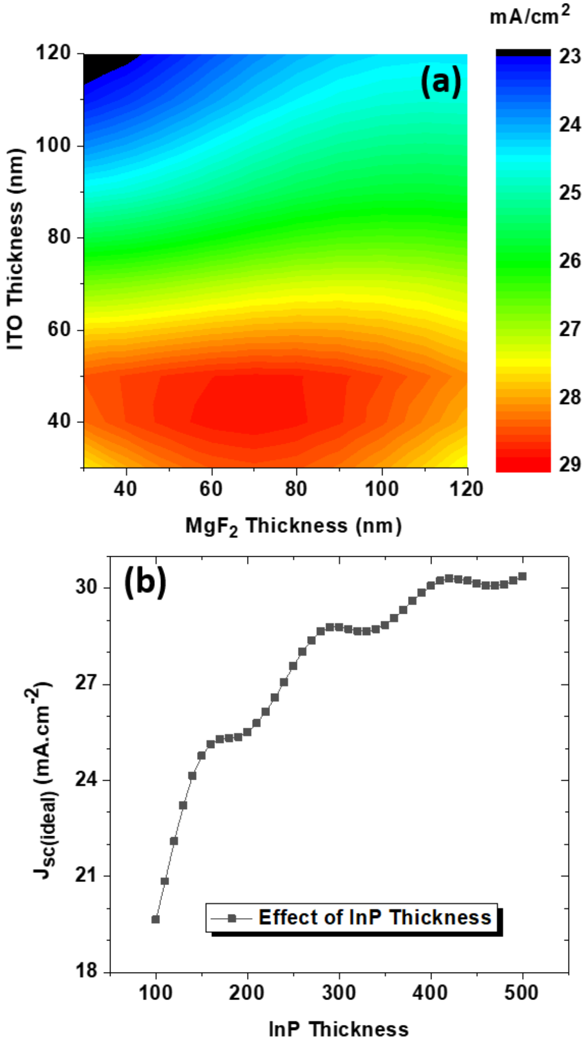

Fig. 2. (a) $J_{sc(ideal)}$ as a function of MgF_2 and ITO thickness. (b) Effect of InP thickness on $J_{sc(ideal)}$ in the presence of an optimum anti-reflective coating and metal back reflector.

III. RESULTS

A. Optical Simulation

A 2-D FDTD simulation was performed to study the effect of thickness of InP on $J_{sc(ideal)}$ in the presence of a metal back reflector and a top anti-reflection coating. The anti-reflective coating comprises of a stack of ZnO, ITO, and MgF_2, whereas, the metal back reflector is a one µm-thick Cu film. For optimization of anti-reflective coating, the thickness of ZnO is fixed at 10 nm while those of ITO and MgF_2, are varied to achieve minimum reflection from the top surface. We find that the best anti-reflective coating is achieved for 10 nm ZnO, 53 nm ITO, and 80 nm MgF_2. Using the optimized anti-reflective coating, reflection from the front of the cell decreases below 10% for most of the wavelength regime, leading to a $J_{sc(ideal)}$ greater than 28 mA/cm^2 for InP thickness as low as 280 nm. Figure 2(a) shows the effect of the thickness of MgF_2 and ITO on the $J_{sc(ideal)}$ of the proposed solar cell when the thickness of InP is fixed at 280 nm.

We next calculate the maximum J_{sc} that can be obtained from InP thin film of different thicknesses. Figure 2(b) shows the effect of InP thickness on the $J_{sc(ideal)}$ of the solar cell in the presence of an optimum anti-reflective coating and a metal back reflector. The $J_{sc(ideal)}$ shows an oscillatory behavior depending on the thickness of InP because of optical resonance and interference effects, consistent with previously reported J_{sc} behavior for thin film heterojunction solar cells [54-56]. The ideal short circuit current has three local maxima for three different InP thicknesses. The maxima occur at an InP thickness of 170, 280 and 430 nm. It is evident that the degree of $J_{sc(ideal)}$ reduces with increasing InP thickness. For example, a gain of ~9.5 mA/cm^2 is achieved when InP thickness is increased from 100 to 280 nm; however, this gain reduces to less than 2 mA/cm^2 when the thickness is further increased from 280 to 460 nm. The decrease in the influence of InP thickness on $J_{sc(ideal)}$ is a result of reduced impact of optical confinement with increased thickness of InP, as confirmed by plotting the generation rate for different InP thicknesses shown in Fig. 3. In general, the generation rate vs. depth curve for a solar cell is an exponentially decaying curve. However, in the current solar cell structure, the exponential decay is no longer valid as shown in

Figure 3 because of optical confinement. Figure 3(a)-(d) shows the generation rate plotted against solar cell depth, for different thicknesses of InP. It is apparent from Figure 3 that the effect of optical confinement reduced with increased thickness.

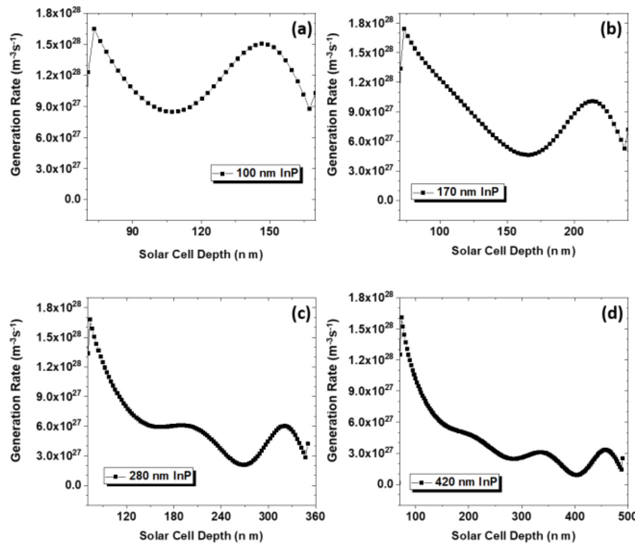

Fig. 3. Carrier generation rate profile for different thicknesses of InP, in presence of an optimized anti-reflective coating and a metal back reflector. (a) 100 nm, (b) 170 nm, (c) 280 nm and (d) 420 nm.

B. *Ideal Condition*

To evaluate the maximum achievable efficiency for our solar cell, we perform device simulation under an ideal condition assuming a bulk minority carrier lifetime of 1 µs (based on ref [57]) and an interface recombination velocity (IRV) of 10^3 cm/s at the InP/CuI and ZnO/InP interfaces. An SRV of the order of 10^3 cm/s has often achieved for both InP [58, 59] as well as oxide/InP [60]. Besides, a thickness of 280 nm of InP is assumed during device simulation, based on optical simulation results obtained above. This means that the current solar cell will also benefit from the photon recycling, as the material thickness if very low. Photon recycling is a proven method for improvement in the V_{oc} of a solar cell device, and has been found crucial in realizing a high V_{oc} of 1.12 V in GaAs solar cells [61, 62]. To investigate the effect of photon recycling, we scale the radiative recombination coefficient according to equation 5. Figure 4(a) shows the IV curves with and without photon recycling. As expected, photon recycling improves the V_{oc} from 1.05 to 1.12 V, while maintaining the J_{sc} and FF at 28.2 mA/cm^2 and 88.3%, respectively. The calculated efficiencies without and with photon recycling are 26.1% and 27.9%, respectively.

The Shockley-Queisser limit (S-Q limit) for InP solar cell predicts a maximum efficiency of ~33.1 % with a V_{oc}, J_{sc}, and FF of 1.06 V, 33.2 mA/cm^2 and 88.8%, respectively. In comparison to SQ-limit, a slightly lower V_{oc} and FF originates from finite bulk minority carrier lifetime and interface recombination in the proposed solar cell. At the same time, the J_{sc} in proposed device is ~5 mA/cm^2 lower than SQ-limit, mainly because of optical losses. Nonetheless, these optical

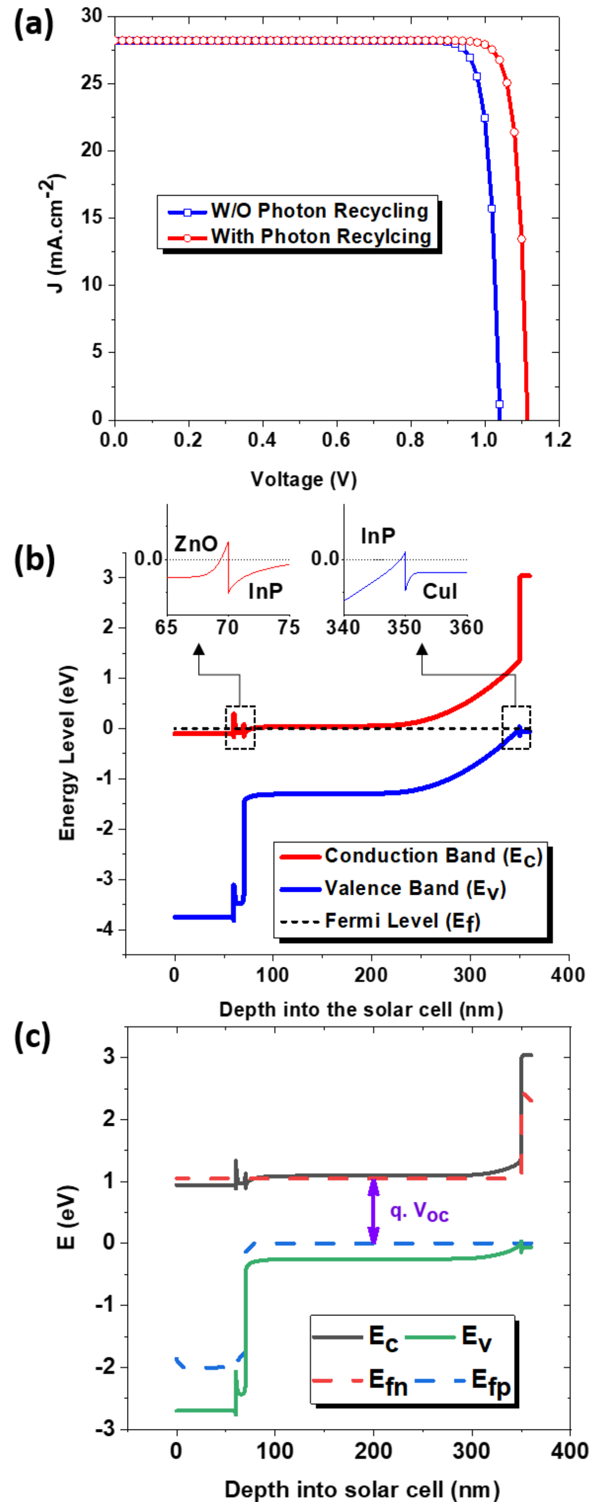

Fig. 4. (a) Simulated J-V curve of the proposed heterojunction solar cell with and without photon recycling, (b) energy band diagram of proposed heterojunction solar cell in dark, and (c) energy band diagram of proposed heterojunction solar cell at V_{oc}.

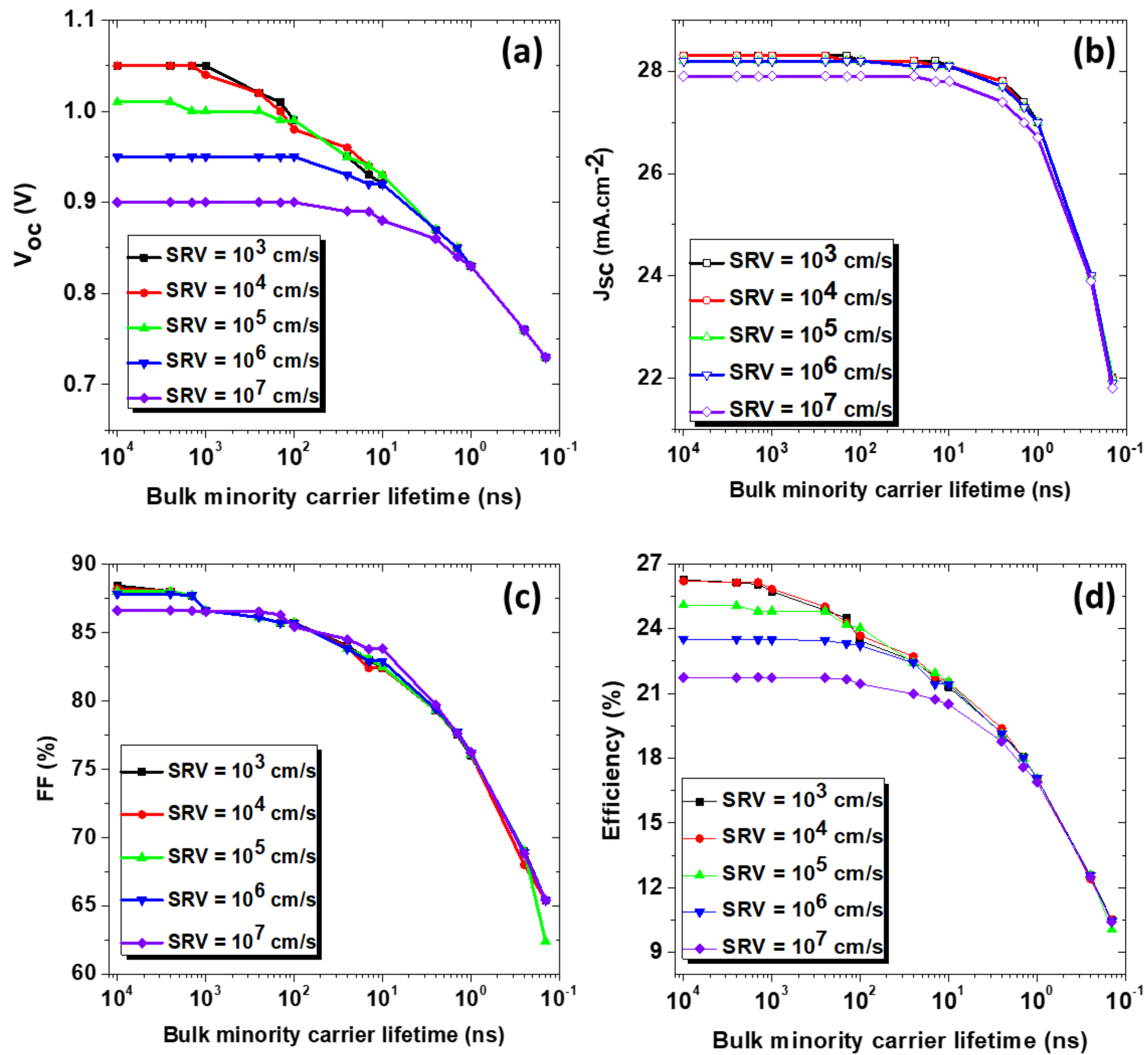

Fig. 5. The effect of bulk defect density and SRV (at CuI/InP and ZnO/InP interface) on (a) V_{oc}, (b) J_{sc}, (c) FF and (d) efficiency of the proposed solar cell.

losses may be reduced in future through utilization of nanostructures and more advanced light trapping techniques [32].

Figure 4(b) shows the band diagram of the proposed device in dark at 0V. InP forms a type-I band alignment with ZnO such that a very small conduction band offset allows unrestricted flow of electrons from InP to ZnO, while a large valence band offset blocks the holes. Similarly, InP band alignment with CuI shows a small valence band offset, and a large conduction band offset which ensures an easy flow of holes from InP to CuI but restricts the flow of electrons. Moreover, previous reports on ZnO and CuI show that both ZnO [2] and CuI [33] are wide band gap material that can be heavily doped relatively easily to achieve high conduction towards electrons and holes, respectively. Therefore, during simulations, we assume both ZnO and CuI are heavily doped with a carrier concentration of $1x10^{19}$ cm^{-3}. Such asymmetric conductivity towards charge carrier is required for carrier selectivity [63, 64]. Furthermore, because of large band gap of ZnO and CuI, there is a very low intrinsic carrier concentration as well as low generation under illumination that ensures that the conductivity of minority carrier always remains extremely low compared to majority carriers, both under dark and under illumination [1, 2, 65]. Therefore, a proper band alignment along with the asymmetric conductivity toward electrons and holes makes both ZnO and CuI perfect candidates for electron and hole selective contact, respectively. In the inset of Figure 4(b) the band bending at InP/CuI and ZnO/InP is shown. It is apparent that at ZnO/InP and InP/CuI interfaces, there is an accumulation of electrons and holes, respectively. Such an accumulation of one kind of charge carrier at the interface has an important consequence toward mitigating the overall effect of interface recombination [66]. Figure 4(c) shows the band diagram of the proposed solar cell under illumination at open circuit voltage. Under steady

state condition, the splitting of electrons and hole quasi-fermi levels at V=V_{oc} is equal to the V_{oc} and is given by relation:

$$q.V_{oc} = (E_{fn} - E_{fp})$$

where, q is the charge of an electron, and $E_{fn}$and E_{fp} are respectively electron and hole quasi-fermi levels. The high V_{oc} in proposed solar cell is also apparent in the band diagram shown in Figure 4(c).

C. Effect of bulk and interface SRH recombination

The Shockley-Read-Hall (SRH) recombination for bulk and interface can respectively be defined in terms of surface recombination velocity and bulk minority carrier lifetime using the equations given below:

$$U_{SRH,I} = \frac{\left(n_{if}p_{if} - n_i^2\right)}{\frac{p_{if} + p_1}{S_n} + \frac{n_{if} + n_1}{S_p}} \qquad 6(a)$$

$$U_{SRH,B} = \frac{(np - n_i^2)}{\tau_p(n + n_1) + \tau_n(p + p_1)} \qquad 6(b)$$

Where,

$$S_n = \sigma_n N_{it} v_{th} \qquad 7(a)$$

$$S_p = \sigma_p N_{it} v_{th} \qquad 7(b)$$

$$\tau_n = \frac{1}{\sigma_n N_t v_{th}} \qquad 8(a)$$

$$\tau_p = \frac{1}{\sigma_p N_t v_{th}} \qquad 8(b)$$

$$p_1 = n_i e^{\frac{E_i - E_T}{k_B T}} \qquad 9(a)$$

$$n_1 = n_i e^{\frac{E_T - E_i}{k_B T}} \qquad 9(b)$$

In the above equations, the parameters *S* with subscript n and p is the surface recombination velocity for the electrons and holes, respectively at the interface. Similarly, σ_n, σ_p , N_{it} and v_{th} are the capture cross-section for electrons, capture cross section for holes, interface trap density, and thermal velocity, respectively. The parameter τ with subscript n and p is the minority carrier lifetimes for the electrons and holes, respectively. To model the SRH recombination, a mid-band gap neutral defect is defined with a capture cross section for electrons as 3 x 10^{-13} cm^2 and for holes as 3 x 10^{-13} cm^2. Further, we vary the interface recombination velocity for CuI/InP and ZnO/InP interfaces from 10^3-10^7 cm/s, while changing the bulk defect density from 10^{11} cm^{-2} to 10^{16} $cm^{-2}eV^{-1}$. By equation 8(a) and 8(b) a change in N_t from 10^{11} to 10^{16} cm^{-2} means that the bulk minority carrier lifetime is varied from 10 μs to 0.1 ns, respectively.

Figure 5(a)-(d) shows the effect of bulk and/or interface SRH recombination on V_{oc}, J_{sc}, FF, and efficiency. As expected, higher bulk and/or interface recombination leads to lower V_{oc} (see Figure 5(a)). Additionally, the effect of photon recycling (not shown here) on V_{oc} is also diminished for higher SRH recombination because most of the excess charge carriers recombine through non-radiative recombination and not thorough radiative recombination. For a bulk minority carrier lifetime (τ_p) of less than 10 ns, changes in SRV seems to have larger effect as compared to when $\tau_p > 10$ ns. Although for τ_p less than 10 ns, the effect of SRV on V_{oc} is minimal, yet the V_{oc} deteriorates significantly because of high bulk recombination. For example, for $\tau_p = 10$ ns, V_{oc} degrades from 1.05 to 0.9 V when the SRV is increased from 10^3 to 10^7 cm/s. On the other hand, for $\tau_p \leq 10$ ns, there is almost no variation in V_{oc} with a change in SRV. Similar trends are obtained for J_{sc} and FF, shown in Figure 5(b) and 5(c), respectively. This shows that for τ_p higher than 10 ns, the solar cell is limited by the bulk recombination, whereas, for τ_p less than 10 ns, the solar cell is limited by interface recombination. In addition, the effect of bulk and interface defect recombination on J_{sc} is almost negligible compared to V_{oc} and FF, especially when τ_p higher than 10 ns. This is because the depletion region extends to a large portion of the solar cell, which allows for highly efficient charge carrier separation and transport through the bulk region of the solar cell. Figure 5(d) shows the effect of bulk and interface defect recombination on the overall efficiency of the solar cell. It is quite clear that the efficiency of proposed solar cell degrades significantly when the τ_p is less than 10 ns, regardless of SRV. Nevertheless, even for bulk minority carrier lifetime of 10 ns and an SRV of 10^5 cm/s, an efficiency of ~22% can be achieved with V_{oc}, J_{sc}, and FF of 0.93V, 28.1 mA/cm^2, 83%, respectively.

IV. DISCUSSION

In this section, we discuss the potential and practicality of the proposed solar cell. At present, III-V semiconductor solar modules may cost anywhere from $40-150/W, which is several orders of magnitude higher than the current prices for mainstream c-Si solar and CdTe modules ($0.30–$0.50/W) [67]. Indeed, the proposed solar cell structure has huge potential to solve several costs related as well as technological challenges of III-V solar cells, especially when combined with low-cost deposition techniques such as TF-VLS (thin-film vapor-liquid-solid) [21-23], CSVT [24, 25](close-spaced vapor transport) and HPVE (hydride vapor phase epitaxy) [68-70]. First of all, these solar cells are extremely thin and therefore reduces the materials cost, which is the most significant component to overall III-V cost [5, 71]. Further, thinner cells allow for higher flexibility and reduce transport and logistics costs. Secondly, the proposed solar cell structure can be particularly important when a controlled formation of p-n homojunction for charge carrier separation can be challenging, such as in the case of

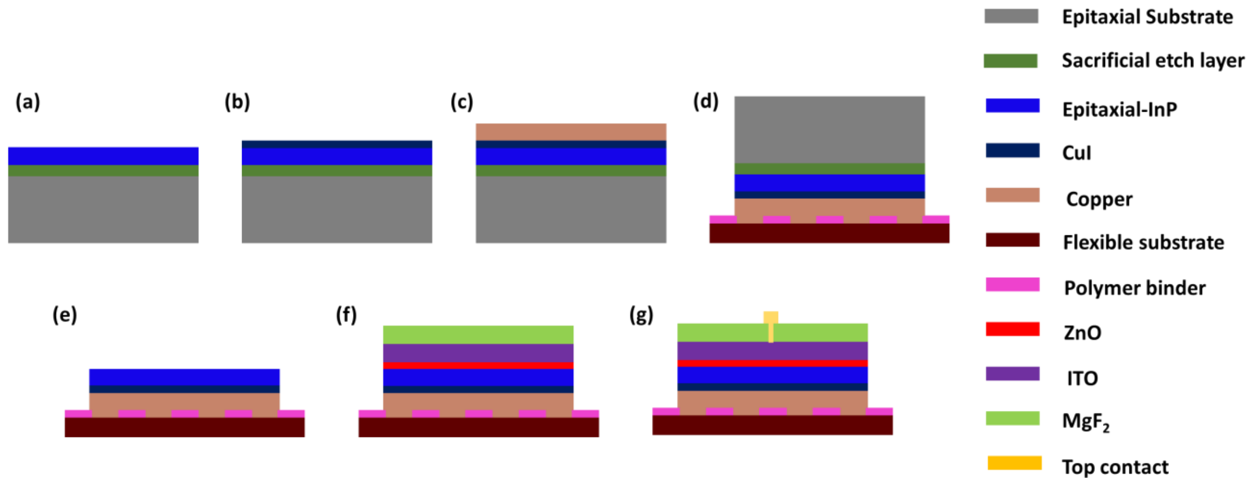

Fig. 6. Proposed fabrication procedure for the solar cell structure with carrier selective contacts: (a) Epitaxial growth of sacrificial layer followed by the growth of absorber layer, (b) Deposition of CuI on epitaxial layer, (c) Deposition of back contact, (d) Binding of wafer with a flexible carrier using a rectangular grid with alternate metal and polymer binder, (e) Selective removal of sacrificial layer, (f) Deposition of ZnO followed by ITO followed by MgF_2, and (g) Deposition of metal contact through MgF_2.

TFVLS and CSVT [22, 23, 25, 72].

In some cases, dopants can lead to degradation of the material quality of the absorber layer, along with additional optoelectronic losses [22, 23, 25]. Because the proposed solar cell structure does not rely on doping of absorber layer, they can overcome several optoelectronic losses while also reducing the complexity and cost associated with doping optimization, especially in case of relatively nascent growth methodology such as TFVLS and CSVT. Another major advantage of the proposed solar cell is that there is no requirement of window layers for passivation, and electron and hole selective contacts are expected to achieve both passivation as well as charge carrier selectivity. Therefore, the proposed solar cell will also reduce the costs associated with doping and growth of window layers. Besides, unlike window layers, the proposed electron and hole selective contacts can respectively be intrinsically heavily n-type and p-type doped at relatively low temperatures. The ease with which these electron and hole selective contacts can be heavily doped has other significant advantages, such as, low contact resistance, high charge carrier selectivity, and reduced interface recombination. In view of the above, the proposed solar cell structure holds vast potential toward achieving high efficiency, low cost flexible InP thin film solar cell.

In addition to several advantages, the proposed solar cells may also have a few limitations and challenges, when compared to very well established homojunction III-V solar cell. One of the biggest challenges would be optimization of carrier selective contacts to achieve both carrier selectivity as well passivation. Though we have shown that ZnO can improve both carrier selectivity as well passivation [1, 2, 32, 34], so far, there is no such study on CuI. Another problem may arise due to instability of copper iodide in ambient atmosphere. Instability of copper iodide has been one of major limitation for its use as in inorganic solar cells [33, 35]. However, in our design, this problem may not be so consequential if copper is deposited over CuI without its exposure to ambient condition. Another big challenge would be transfer and bonding of the proposed solar cell on a flexible or foreign substrate. In conventional solar cell, the layer bonding to metal are very smooth, which reduces the complexity of transfer and bonding to foreign substrate. However, in current case, both ZnO and CuI are expected to have very high roughness and therefore, they cannot be directly transferred and bonded to foreign substrate. One way around this problem would be utilization of grid consisting of alternate layers of polymer binder and metal contact (please see Figure 6). Nonetheless, the proposed solar cell can be realized using a scheme shown in Figure 6.

Figure 6 shows the fabrication scheme that one may adopt to fabricate the proposed device. Fabrication of the proposed device should start with the growth of sacrificial layer and the absorber layer on a lattice matched substrate (Figure 6(a)). After growth of epitaxial layer, a hole selective material should be deposited (Figure 6(b)) followed by deposition of copper for back contact (Figure 6(c)). To bind the wafer coated with back contact (copper) to a flexible carrier, a rectangular grid with alternate metal and polymer binder can be used. A similar scheme has been used by *Chen et al.* to realize more than 19% efficient ultra-thin III-V solar cell [14]. The metal will be required for ohmic contact, whereas the polymer will ensure the wafer bonding. Subsequently, the absorber layer containing the hole selective contact and back contact can be separated from the epitaxial substrate through selective removal of sacrificial layer (Figure 6(e)). After that, ZnO and ITO can be deposited to form the electron selective contact, followed by the deposition of optimum MgF_2 as anti-reflective coating (Figure 6(f)). Finally, the front side can be patterned for metal deposition (Figure 6(g)).

V. Conclusion

We presented heterojunction solar cells based on InP, which

utilize carrier selective contacts for charge carrier separation. We show that an InP thickness as low as 280 nm can achieve a sufficiently high J_{sc} of more than 28 mA/cm^2 in the presence of an optimized anti-reflective coating and a metal back reflector, as a result of optical confinement. Furthermore, a thorough device analysis shows that to achieve sufficiently high efficiency, a bulk lifetime of InP should more than 2 ns while maintaining a surface recombination velocity lower than 10^5 cm/s. Finally, we discuss how our device structure can be important, in cases where doping and growth of p-n junction or window layers are complicated followed by a schematic for realization of the proposed device.

Acknowledgment

This research is supported by the Australian Research Council and Australian National Fabrication Facility is acknowledged for access to simulation tools.

References

[1] V. Raj, L. Fu, H. H. Tan, and C. Jagadish, “Design Principles for Fabrication of InP-Based Radial Junction Nanowire Solar Cells Using an Electron Selective Contact,” *IEEE J. Photovolt.,* vol. 9, no. 4, pp. 980-991, 2019. https://doi.org/10.1109/JPHOTOV.2019.2911157.

[2] V. Raj, T. S. d. Santos, F. Rougieux, K. Vora, M. Lysevych, L. Fu, S. Mokkapati, H. H. Tan, and C. Jagadish, “Indium phosphide based solar cell using ultra-thin ZnO as an electron selective layer,” *J. Phys. D: Appl. Phys.,* vol. 51, no. 39, pp. 395301, 2018. https://doi.org/10.1088/1361-6463/aad7e3.

[3] J. S. Ward, T. Remo, K. Horowitz, M. Woodhouse, B. Sopori, K. VanSant, and P. Basore, “Techno-economic analysis of three different substrate removal and reuse strategies for III-V solar cells,” *Prog. Photov.,* vol. 24, no. 9, pp. 1284-1292, 2016. https://doi.org/10.1002/pip.2776.

[4] A. L. Greenaway, J. W. Boucher, S. Z. Oener, C. J. Funch, and S. W. Boettcher, “Low-Cost Approaches to III–V Semiconductor Growth for Photovoltaic Applications,” *ACS Energy Lett.,* vol. 2, no. 10, pp. 2270-2282, 2017. https://doi.org/10.1021/acsenergylett.7b00633.

[5] J. Simon, L. K. Schulte, A. K. Horowitz, T. Remo, L. D. Young, and J. A. Ptak, “III-V-Based Optoelectronics with Low-Cost Dynamic Hydride Vapor Phase Epitaxy,” *Crystals,* vol. 9, no. 1, 2018. https://doi.org/10.3390/cryst9010003.

[6] K. Sun, A. Kargar, N. Park, K. N. Madsen, P. W. Naughton, T. Bright, Y. Jing, and D. L. Wang, “Compound Semiconductor Nanowire Solar Cells,” *IEEE J. Sel. Top. Quantum Electron.,* vol. 17, no. 4, pp. 1033-1049, 2011. https://doi.org/10.1109/jstqe.2010.2090342.

[7] P. Demeester, I. Pollentier, P. D. Dobbelaere, C. Brys, and P. V. Daele, “Epitaxial lift-off and its applications,” *Semiconductor Science and Technology,* vol. 8, no. 6, pp. 1124-1135, 1993. https://doi.org/10.1088/0268-1242/8/6/021.

[8] C.-W. Cheng, K.-T. Shiu, N. Li, S.-J. Han, L. Shi, and D. K. Sadana, “Epitaxial lift-off process for gallium arsenide substrate reuse and flexible electronics,” *Nature Comm.,* vol. 4, pp. 1577, 2013. https://doi.org/10.1038/ncomms2583.

[9] T. R. Kelsey A. W. Horowitz, Brittany Smith, and Aaron Ptak, *A Techno-Economic Analysis and Cost Reduction Roadmap for III-V Solar Cells*, National Renewable Energy Laboratory, Golden, Colarado, USA, 2018. https://doi.org/10.2172/1484349.

[10] W. Yang, J. Becker, S. Liu, Y.-S. Kuo, J.-J. Li, B. Landini, K. Campman, and Y.-H. Zhang, “Ultra-thin GaAs single-junction solar cells integrated with a reflective back scattering layer,” *J. Appl. Phys.,* vol. 115, no. 20, pp. 203105, 2014/05/28, 2014. https://doi.org/10.1063/1.4878156.

[11] A. Freundlich, A. Mehrotra, M. Gunasekera, G. Lancel, and G. K. Vijaya, "Ultra-thin defect tolerant high efficiency III–V tandems for development of low-cost photovoltaics." pp. 2117-2121. Presented at 2014 IEEE 40th Photovoltaic Specialist Conference (PVSC), [Online]. Available: https://doi.org/10.1109/PVSC.2014.6925342.

[12] S. Eyderman, and S. John, “Light-trapping and recycling for extraordinary power conversion in ultra-thin gallium-arsenide solar cells,” *Sci. Rep.,* vol. 6, pp. 28303, 2016. https://doi.org/10.1038/srep28303.

[13] F. Proulx, M. C. A. York, P. O. Provost, R. Arès, V. Aimez, D. P. Masson, and S. Fafard, “Measurement of strong photon recycling in ultra-thin GaAs n/p junctions monolithically integrated in high-photovoltage vertical epitaxial heterostructure architectures with conversion efficiencies exceeding 60%,” *Phys. Status Solidi RRL,* vol. 11, no. 2, pp. 1600385, 2017. https://doi.org/10.1002/pssr.201600385.

[14] H.-L. Chen, A. Cattoni, R. De Lépinau, A. W. Walker, O. Höhn, D. Lackner, G. Siefer, M. Faustini, N. Vandamme, J. Goffard, B. Behaghel, C. Dupuis, N. Bardou, F. Dimroth, and S. Collin, “A 19.9%-efficient ultrathin solar cell based on a 205-nm-thick GaAs absorber and a silver nanostructured back mirror,” *Nature Energy*, vol. 4, pp. 761-767, 2019. https://doi.org/10.1038/s41560-019-0434-y.

[15] E. D. Kosten, J. H. Atwater, J. Parsons, A. Polman, and H. A. Atwater, “Highly efficient GaAs solar cells by limiting light emission angle,” *Light Sci. Appl.,* vol. 2, pp. e45, 2013. https://doi.org/10.1038/lsa.2013.1.

[16] Z. Ren, M. Thway, Z. Liu, Y. Wang, C. Ke, K. N. Yaung, B. Wang, C. S. Tan, F. Lin, A. G. Aberle, T. Buonassisi, and I. M. Peters, “Ultra-Thin GaAs Double-Junction Solar Cell With Carbon-Doped Emitter,” *IEEE J. Photovolt.,* vol. 8, no. 6, pp. 1627-1634, 2018. https://doi.org/10.1109/JPHOTOV.2018.2870721.

[17] S.-M. Lee, A. Kwong, D. Jung, J. Faucher, R. Biswas, L. Shen, D. Kang, M. L. Lee, and J. Yoon, “High Performance Ultrathin GaAs Solar Cells Enabled with Heterogeneously Integrated Dielectric Periodic Nanostructures,” *ACS Nano,* vol. 9, no. 10, pp. 10356-10365, 2015/10/27, 2015. https://doi.org/10.1021/acsnano.5b05585.

[18] B. Gai, Y. Sun, H. Lim, H. Chen, J. Faucher, M. L. Lee, and J. Yoon, “Multilayer-Grown Ultrathin Nanostructured GaAs Solar Cells as a Cost-Competitive Materials Platform for III–V Photovoltaics,” *ACS Nano,* vol. 11, no. 1, pp. 992-999, 2017/01/24, 2017. https://doi.org/10.1021/acsnano.6b07605.

[19] J. Bullock, M. Hettick, J. Geissbühler, A. J. Ong, T. Allen, Carolin M. Sutter-Fella, T. Chen, H. Ota, E. W. Schaler, S. De Wolf, C. Ballif, A. Cuevas, and A. Javey, “Efficient silicon solar cells with dopant-free asymmetric heterocontacts,” *Nature Energy,* vol. 1, pp. 15031, 2016. https://doi.org/10.1038/nenergy.2015.31

[20] A. Goodrich, and M. Woodhouse, *A Manufacturing Cost Analysis Relevant to Single- and Dual-Junction Photovoltaic Cells Fabricated with III-Vs and III-Vs Grown on Czochralski Silicon*, National Renewable Energy Laboratory (NREL), Colarado, United States, 2013. https://doi.org/10.2172/1336550.

[21] M. Zheng, K. Horowitz, M. Woodhouse, C. Battaglia, R. Kapadia, and A. Javey, “III-Vs at scale: a PV manufacturing cost analysis of the thin film vapor–liquid–solid growth mode,” *Progress in Photovoltaics: Research and Applications,* vol. 24, no. 6, pp. 871-878, 2016. https://doi.org/10.1002/pip.2740.

[22] R. Kapadia, Z. Yu, H.-H. H. Wang, M. Zheng, C. Battaglia, M. Hettick, D. Kiriya, K. Takei, P. Lobaccaro, J. W. Beeman, J. W. Ager, R. Maboudian, D. C. Chrzan, and A. Javey, “A direct thin-film path towards low-cost large-area III-V photovoltaics,” *Sci. Rep.,* vol. 3, pp. 2275, 2013. https://doi.org/10.1038/srep02275.

[23] Y. Sun, X. Sun, S. Johnston, C. M. Sutter-Fella, M. Hettick, A. Javey, and P. Bermel, "Voc degradation in TF-VLS grown InP solar cells." pp. 1934-1937. Presented at 2016 IEEE 43rd Photovoltaic Specialists Conference (PVSC), [Online]. Available: https://doi.org/10.1109/PVSC.2016.7749962.

[24] A. J. Ritenour, R. C. Cramer, S. Levinrad, and S. W. Boettcher, “Efficient n-GaAs Photoelectrodes Grown by Close-Spaced Vapor

Transport from a Solid Source," *ACS Appl. Mater. Interfaces,* vol. 4, no. 1, pp. 69-73, 2012. https://doi.org/10.1021/am201631p.

[25] A. J. Ritenour, J. W. Boucher, R. DeLancey, A. L. Greenaway, S. Aloni, and S. W. Boettcher, "Doping and electronic properties of GaAs grown by close-spaced vapor transport from powder sources for scalable III–V photovoltaics," *Energy Environ. Sci.,* vol. 8, no. 1, pp. 278-285, 2015. https://doi.org/10.1039/C4EE01943A.

[26] J. Bullock, Y. Wan, M. Hettick, X. Zhaoran, S. P. Phang, D. Yan, H. Wang, W. Ji, C. Samundsett, Z. Hameiri, D. Macdonald, A. Cuevas, and A. Javey, "Dopant-Free Partial Rear Contacts Enabling 23% Silicon Solar Cells," *Adv. Energy Mater.,* vol. 9, no. 9, pp. 1803367, 2019. https://doi.org/10.1002/aenm.201803367.

[27] S. Z. Oener, A. Cavalli, H. Sun, J. E. M. Haverkort, E. P. A. M. Bakkers, and E. C. Garnett, "Charge carrier-selective contacts for nanowire solar cells," *Nature Comm.,* vol. 9, no. 1, pp. 3248, 2018. https://doi.org/10.1038/s41467-018-05453-5.

[28] X. Yin, C. Battaglia, Y. Lin, K. Chen, M. Hettick, M. Zheng, C.-Y. Chen, D. Kiriya, and A. Javey, "19.2% Efficient InP Heterojunction Solar Cell with Electron-Selective TiO2 Contact," *ACS Photonics,* vol. 1, no. 12, pp. 1245-1250, 2014. https://doi.org/10.1021/ph500153c.

[29] P. R. Narangari, S. K. Karuturi, Y. Wu, J. Wong-Leung, K. Vora, M. Lysevych, Y. Wan, H. H. Tan, C. Jagadish, and S. Mokkapati, "Ultrathin Ta2O5 electron-selective contacts for high efficiency InP solar cells," *Nanoscale,* vol. 11, no. 15, pp. 7497-7505, 2019. https://doi.org/10.1039/C8NR09932D.

[30] V. Raj, P. Balaji, M. Joshi, and M. Kumar, "Ag Grafted ZnO Nanoplates for Photocatalytic Applications," *Mater. Focus,* vol. 3, no. 5, pp. 385-391, 2014. https://doi.org/10.1166/mat.2014.1192.

[31] M. Joshi, V. Raj, P. S. Balaji, and A. Kaushik, "Ag–ZnO Nanocomposite for Multi Gas Sensing Applications." Jain V., Verma A. (eds) Physics of Semiconductor Devices. Environmental Science and Engineering. Springer, Cham, pp. 453-456. https://doi.org/10.1007/978-3-319-03002-9_113.

[32] V. Raj, K. Vora, L. Fu, H. H. Tan, and C. Jagadish, "High-Efficiency Solar Cells from Extremely Low Minority Carrier Lifetime Substrates Using Radial Junction Nanowire Architecture," *ACS Nano*, 2019/09/20, 2019. https://doi.org/10.1021/acsnano.9b06226.

[33] V. Raj, T. Lu, M. Lockrey, R. Liu, F. Kremer, L. Li, Y. Liu, H. H. Tan, and C. Jagadish, "Introduction of TiO2 in CuI for Its Improved Performance as a p-Type Transparent Conductor," *ACS Appl. Mater. Interfaces,* vol. 11, no. 27, pp. 24254-24263, 2019. https://doi.org/10.1021/acsami.9b05566.

[34] V. Raj, K. Vora, L. Li, L. Fu, H. H. Tan, and C. Jagadish, "Electron selective contact for high efficiency core-shell nanowire solar cell." pp. 1-1. Presented at 2019 Compound Semiconductor Week (CSW). [Online]. Available: https://doi.org/10.1109/ICIPRM.2019.8819194

[35] V. Raj, M. Lockrey, R. Liu, H. H. Tan, and C. Jagadish, "CuI-TiO2 Composite Thin Film for Flexible Electronic Applications." pp. 22-23. Presented at 2018 Conference on Optoelectronic and Microelectronic Materials and Devices (COMMAD). [Online]. Available: https://doi.org/10.1109/COMMAD.2018.8715246.

[36] May 2019; http://www.lumerical.com/tcad-products/fdtd/.

[37] D. M. Sullivan, "One-Dimensional Simulation with the FDTD Method," in *Electromagnetic Simulation Using the FDTD Method*, 2013. https://doi.org/doi:10.1002/9781118646700.ch1

[38] M. Burgelman, P. Nollet, and S. Degrave, "Modelling polycrystalline semiconductor solar cells," *Thin Solid Films,* vol. 361-362, pp. 527-532, 2000. https://doi.org/https://doi.org/10.1016/S0040-6090(99)00825-1.

[39] K. D. Marc Burgelman, Alex Niemegeers, Johan Verschraegen, Stefaan Degrave, *SCAPS manual*, Belgium, 13 february 2019.

[40] S. R. Lunt, G. N. Ryba, P. G. Santangelo, and N. S. Lewis, "Chemical studies of the passivation of GaAs surface recombination using sulfides and thiols," *J. Appl. Phys.,* vol. 70, no. 12, pp. 7449-7467, 1991. https://doi.org/10.1063/1.349741.

[41] O. Madelung, U. Rössler, and M. Schulz, "Cuprous iodide (gamma-CuI) dielectric constants, refractive index: Datasheet from Landolt-Börnstein - Group III Condensed Matter · Volume 41B: "II-VI and I-VII Compounds; Semimagnetic Compounds" in SpringerMaterials ": Springer-Verlag Berlin Heidelberg, 1999.

[42] A. Martí, J. L. Balenzategui, and R. F. Reyna, "Photon recycling and Shockley's diode equation," *J. Appl. Phys.,* vol. 82, no. 8, pp. 4067-4075, 1997. https://doi.org/10.1063/1.365717.

[43] T. Kirchartz, F. Staub, and U. Rau, "Impact of Photon Recycling on the Open-Circuit Voltage of Metal Halide Perovskite Solar Cells," *ACS Energy Lett.,* vol. 1, no. 4, pp. 731-739, 2016. https://doi.org/10.1021/acsenergylett.6b00223.

[44] T. P. Xiao, G. Scranton, V. Ganapati, J. Holzrichter, P. Peterson, and E. Yablonovitch, "Enhancing the Efficiency of Thermophotovoltaics with Photon Recycling," Presented at *2016* Conference on Lasers and Electro-Optics (CLEO). [Online]. Available: https://doi.org/10.1364/CLEO_AT.2016.ATu1K.2.

[45] X. Wang, M. R. Khan, J. L. Gray, M. A. Alam, and M. S. Lundstrom, "Design of GaAs Solar Cells Operating Close to the Shockley–Queisser Limit," *IEEE J. Photovolt.,* vol. 3, no. 2, pp. 737-744, 2013. https://doi.org/10.1109/JPHOTOV.2013.2241594.

[46] J. E. Parrott, "Radiative recombination and photon recycling in photovoltaic solar cells," *Sol. Energy Mater. Sol. Cells,* vol. 30, no. 3, pp. 221-231, 1993. https://doi.org/https://doi.org/10.1016/0927-0248(93)90142-P.

[47] M. P. Lumb, M. A. Steiner, J. F. Geisz, and R. J. Walters, "Incorporating photon recycling into the analytical drift-diffusion model of high efficiency solar cells," *J. Appl. Phys.,* vol. 116, no. 19, pp. 194504, 2014. https://doi.org/10.1063/1.4902320.

[48] P. Asbeck, "Self-absorption effects on the radiative lifetime in GaAs-GaAlAs double heterostructures," *J. Appl. Phys.,* vol. 48, no. 2, pp. 820-822, 1977. https://doi.org/10.1063/1.323633.

[49] J. W. Parks, K. F. Brennan, and A. W. Smith, "Two-dimensional model of photon recycling in direct gap semiconductor devices," *J. Appl. Phys.,* vol. 82, no. 7, pp. 3493-3498, 1997. https://doi.org/10.1063/1.365622.

[50] Y. Sun, A. Perna, and P. Bermel, "Comparing Front- and Rear-Junction GaInP Photovoltaic Devices Through Detailed Numerical and Analytical Modeling," *IEEE J. Photovolt.,* vol. 9, no. 2, pp. 437-445, 2019. https://doi.org/10.1109/JPHOTOV.2019.2892530.

[51] S. Luryi, and A. Subashiev, "Lévy flight of holes in inp semiconductor scintillator," *International Journal of High Speed Electronics and Systems,* vol. 21, no. 01, pp. 1250001, 2012. https://doi.org/10.1142/S0129156412500012.

[52] X. D. Chen, N. F. Sun, T. N. Sun, S. L. Liu, G. Y. Yang, Y. W. Zhao, X. L. Xu, C. D. Beling, and S. Fung, "Electrical and FT-IR measurements of undoped n-type InP materials grown from various stoichiometric melts." pp. 42-44. Presented at 1998 International Conference on Indium Phosphide and Related Materials (Cat. No.98CH36129). [Online]. Available: https://doi.org/10.1109/ICIPRM.1998.712396.

[53] R. Hirano, and T. Kanazawa, "Heat treatments of InP wafers," *J. Cryst. Growth,* vol. 106, no. 4, pp. 531-536, 1990. https://doi.org/https://doi.org/10.1016/0022-0248(90)90026-H.

[54] H. Y. Chunfu Zhang, Yue Hao, Zhenhua Lin and Chunxiang Zhu, "Solar Cells - New Aspects and Solutions," *Effects of Optical Interference and Annealing on the Performance of Polymer/Fullerene Bulk Heterojunction Solar Cells*, L. A. Kosyachenko, ed., pp. 1-27: InTechOpen, 2011.

[55] H. Hoppe, S. Shokhovets, and G. Gobsch, "Inverse relation between photocurrent and absorption layer thickness in polymer solar cells," *physica status solidi (RRL) – Rapid Research Letters,* vol. 1, no. 1, pp. R40-R42, 2007/01/01, 2007. https://doi.org/10.1002/pssr.200600011.

[56] J. Cao, Z. Zhan, L. Hou, Y. Long, P. Liu, and W. Mai, "Optical modeling of organic solar cells based on rubrene and C70," *Applied Optics,* vol. 51, no. 23, pp. 5718-5723, 2012/08/10, 2012. https://doi.org/10.1364/AO.51.005718.

[57] Author ed.^eds., "Properties, Processing and Applications of Indium Phosphide," *Minority-carrier lifetime of InP*, London, United Kingdom: INSPEC, The Institution of Electrical Engineers, 2000, p.^pp. Pages.

[58] Y. Rosenwaks, Y. Shapira, and D. Huppert, "Evidence for low intrinsic surface-recombination velocity onp-type InP," *Physical Review B,* vol. 44, no. 23, pp. 13097-13100, 1991. https://doi.org/10.1103/physrevb.44.13097.

[59] Y. Rosenwaks, Y. Shapira, and D. Huppert, "Picosecond time-resolved luminescence studies of surface and bulk recombination

processes in InP," *Physical Review B,* vol. 45, no. 16, pp. 9108-9119, 1992. https://doi.org/10.1103/physrevb.45.9108.
[60] L. E. Black, A. Cavalli, M. A. Verheijen, J. E. M. Haverkort, E. P. A. M. Bakkers, and W. M. M. Kessels, "Effective Surface Passivation of InP Nanowires by Atomic-Layer-Deposited Al2O3 with POx Interlayer," *Nano Lett.,* vol. 17, no. 10, pp. 6287-6294, 2017/10/11, 2017. https://doi.org/10.1021/acs.nanolett.7b02972.
[61] B. M. Kayes, H. Nie, R. Twist, S. G. Spruytte, F. Reinhardt, I. C. Kizilyalli, and G. S. Higashi, "27.6% Conversion efficiency, a new record for single-junction solar cells under 1 sun illumination." pp. 000004-000008.
[62] O. D. Miller, E. Yablonovitch, and S. R. Kurtz, "Strong Internal and External Luminescence as Solar Cells Approach the Shockley–Queisser Limit," *IEEE J. Photovolt.,* vol. 2, no. 3, pp. 303-311, 2012. https://doi.org/10.1109/JPHOTOV.2012.2198434.
[63] R. Brendel, and R. Peibst, "Contact Selectivity and Efficiency in Crystalline Silicon Photovoltaics," *IEEE J. Photovolt.,* vol. 6, no. 6, pp. 1413-1420, 2016. https://doi.org/10.1109/JPHOTOV.2016.2598267.
[64] S. W. Glunz, M. Bivour, C. Messmer, F. Feldmann, R. Müller, C. Reichel, A. Richter, F. Schindler, J. Benick, and M. Hermle, "Passivating and Carrier-selective Contacts - Basic Requirements and Implementation." pp. 2064-2069.
[65] U. Würfel, A. Cuevas, and P. Würfel, "Charge Carrier Separation in Solar Cells," *IEEE J. Photovolt.,* vol. 5, no. 1, pp. 461-469, 2015. https://doi.org/10.1109/JPHOTOV.2014.2363550.
[66] A. Niemegeers, M. Burgelman, and A. De Vos, "On the CdS/CuInSe2 conduction band discontinuity," *Appl. Phys. Lett.,* vol. 67, no. 6, pp. 843-845, 1995. https://doi.org/10.1063/1.115523.
[67] T. R. Kelsey A. W. Horowitz, Brittany Smith, and Aaron Ptak, *Techno-Economic Analysis and Cost Reduction Roadmap for III-V Solar Cells*, National Renewable Energy Laboratory, Golden, CO, USA, 2018.
[68] J. Simon, K. L. Schulte, N. Jain, S. Johnston, M. Young, M. R. Young, D. L. Young, and A. J. Ptak, "Upright and Inverted Single-Junction GaAs Solar Cells Grown by Hydride Vapor Phase Epitaxy," *IEEE J. Photovolt.,* vol. 7, no. 1, pp. 157-161, 2017. https://doi.org/10.1109/JPHOTOV.2016.2614122.
[69] J. Simon, D. Young, and A. Ptak, "Low-cost III–V solar cells grown by hydride vapor-phase epitaxy." pp. 0538-0541. Presented at 2014 IEEE 40th Photovoltaic Specialist Conference (PVSC). [Online]. Available: https://doi.org/10.1109/PVSC.2014.6924977.
[70] W. Metaferia, K. L. Schulte, J. Simon, S. Johnston, and A. J. Ptak, "Gallium arsenide solar cells grown at rates exceeding 300 µm h(-1) by hydride vapor phase epitaxy," *Nature communications,* vol. 10, no. 1, pp. 3361-3361, 2019. https://doi.org/10.1038/s41467-019-11341-3.
[71] J. W. Boucher, A. J. Ritenour, A. L. Greenaway, S. Aloni, and S. W. Boettcher, "Homojunction GaAs solar cells grown by close space vapor transport." pp. 0460-0464. Presented at 2014 IEEE 40th Photovoltaic Specialist Conference (PVSC). [Online]. Available: https://doi.org/10.1109/PVSC.2014.6924959

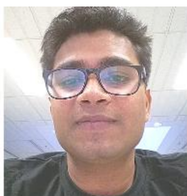

Vidur Raj (M'16) received his B.Tech+M.tech (Dual Degree) in nanotechnology from Amity Universty, Noida, India, in 2014. Currently, he is working toward his Ph.D. degree in physics under the supervision of Prof. Hoe Tan, Prof. Lan Fu, Dr Fiacre Rougieux, and Prof. Chennupati Jagadish at The Australian National University, Canberra, Australia. His topic of Ph.D. is "Optoelectronic Simulation and Fabrication of Thin Flim/Nanowire Heterojunction Solar Cells based on InP".

Fiacre Rougieux received a PhD degree from the Australian National University, Canberra in 2012. He joined the University of New South Wales, Sydney Australia in 2018 where he leads research on materials for high-efficiency solar cells and advanced optoelectronics devices. His current work lies at the intersection of materials science, nanotechnology, solid-state chemistry, solar cells and semiconductor physics. Between 2012 and 2015, he was an ARENA Post-doctoral Fellow at the Australian National University where he developed high-efficiency and low-cost solar cell concepts. One of the outcomes of his research was three consecutive world efficiency records for solar cells made with Updgraded Metallurgical Grade silicon. Between 2016 and 2019, he was an ARC DECRA fellow at the ANU and UNSW where he explored the physics of defects in high efficiency devices and successfully developed a wide range of processes to remove defects in solar cells and improve their efficiency.

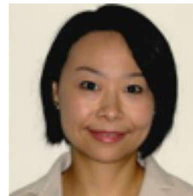

Lan Fu (SM'07) received the M.Sc. degree from the University of Science and Technology of China, Hefei, China, in 1996 and the Ph.D. degree from The Australia National University, Canberra, Australia, in 2001. She is currently a Professor the Department of Electronic Materials Engineering, The Australia National University. Her main research interests include the design, fabrication, and integration of optoelectronic devices (lasers and photodetectors) and high-efficiency solar cells based on low-dimensional III–V compound semiconductor structures, including quantum wells, self-assembled quantum dots, and nanowires grown by metal-organic chemical vapor deposition (MOCVD).

Hark Hoe Tan (SM'14-F'19) received the B.Eng. (Hons.) degree in electrical engineering from the University of Melbourne in 1992, after which he worked with Osram in Malaysia as a Quality Assurance Engineer. In 1997, he received the PhD degree from The Australian National University for his dissertation entitled "Ion beam effects in GaAs/AlGaAs material and devices." He has been the past recipient of the Australian Research Council Postdoctoral, QEII and Future Fellowships. He has published/co-published over 400 journal papers and 6 book chapters, and is a co-inventor in 4 US patents related to laser diodes and infrared photodetectors. His research interests include epitaxial growth of low-dimensional compound semiconductors, nanostructured optoelectronic devices and ion-implantation processing of compound semiconductors for optoelectronic device applications. Prof. Tan has been elected as a Fellow of the IEEE from 2019 and was the Distinguished Lecturer for IEEE Nanotechnology Council (2016 & 2017) and IEEE Photonics Society (2016-2017). He has been the past chair of the Photonics Society, Electron Devices Society and Nanotechnology Council chapters of the IEEE ACT section.

Chennupati Jagadish AC (F'02) is a Distinguished Professor and Head of Semiconductor Optoelectronics and Nanotechnology Group in the Research School of Physics and Engineering, Australian National University. He has served as Vice-President and Secretary Physical Sciences of the Australian Academy of Science during 2012-2016. He is currently serving as President of IEEE Photonics Society, and President of Australian Materials Research Society. His research interests include optoelectronics nanotechnology and neuroscience. Prof. Jagadish is an Editor/Associate editor of 6 Journals (EIC: Progress in Quantum Electronics), 3 book series and serves on editorial boards of 20 other journals. He has published more than 900 research papers (620 journal papers), holds 5 US patents, co-authored a book, co-edited 12 books and edited 12 conference proceedings and 17 special issues of Journals. He is a Fellow of 8 Science and Engineering Academies (the Australian Academy of Science, Australian Academy of Technological Sciences and Engineering, The World Academy of Sciences, US National Academy of Inventors, Indian National Science Academy (Foreign Fellow), Indian National Academy of Engineering (Foreign Fellow), Indian Academy of

Science (Honorary Fellow), Andhra Pradesh Akademi of Sciences (Honorary Fellow)) and a Fellow of 14 Professional Societies (IEEE, APS, MRS, OSA, AVS, ECS, SPIE, AAAS, FEMA, APAM, IoP (UK), IET (UK), IoN (UK) and the AIP). He received Peter Baume Award from the ANU in 2006, the Quantum Device Award from ISCS in 2010, Electronics and Photonics Division Award of the Electrochemical Society in 2012, 2013 Walter Boas Medal, 2015 IEEE Pioneer Award in Nanotechnology, 2015 IEEE Photonics Society Engineering Achievement Award, 2016 MRSI Silver Jubilee Anniversary Medal, 2016 Distinguished Fellow of Chinese Academy of Sciences, 2016 OSA Nick Holonyak Award, 2017 Welker Award, 2017 IUMRS Somiya Award, 2017 Nayudamma Award, 2018 AVS Nanotechnology Recognition Award and 2018 UNESCO Medal for contributions to the development of nanoscience and nanotechnologies. He has received Australia's highest civilian honor, AC, Companion of the Order of Australia in 2016 for his contribution to Physics and Engineering, in particular Nanotechnology.